J. Microbiol. Biotechnol. (2011), **21**(1), 28–36
doi: 10.4014/jmb.1007.07041
First published online 19 November 2010

JOURNAL OF MICROBIOLOGY AND BIOTECHNOLOGY

Amphotericin B Aggregation Inhibition with Novel Nanoparticles Prepared with Poly(ε-caprolactone)/Poly(*N*,*N*-dimethylamino-2-ethyl methacrylate) Diblock Copolymer

Shim, Yong-Ho[1,2], You-Chan Kim[3], Hong-Joo Lee[4], Francois Bougard[1], Philippe Dubois[1], Ki-Choon Choi[5], Chung-Wook Chung[6], Dae Hwan Kang[6]*, and Young-Il Jeong[6]*

[1]*Laboratory of Polymeric and Composite Materials, Center for Innovation and Research in Materials and Polymers (CIRMAP), University of Mons-Hainaut, Place du Parc 20, Mons, 7000, Belgium*
[2]*Korea–Europe Technology Center, Seoul 158-072, Korea*
[3]*Department of Food Science and Biotechnology, Sungkyunkwan University, Suwon 440-746, Korea*
[4]*Gwangju Development Institute, Gwangju 506-042, Korea*
[5]*Grassland and Forages Research Center, National Institute of Animal Science, Rural Development Administration, Chungnam 331-808, Korea*
[6]*National Research and Development Center for Hepatobiliary Disease, Pusan National University Yangsan Hospital, Gyeongnam 626-770, Korea*

Received: July 20, 2010 / Revised: October 6, 2010 / Accepted: October 25, 2010

Diblock copolymers composed of poly(ε-caprolactone) (PCL) and poly(*N*,*N*-dimethylamino-2-ethyl methacrylate) (PDMAEMA), or methoxy polyethylene glycol(PEG), were synthesized *via* a combination of ring-opening polymerization and atom-transfer radical polymerization in order to prepare polymeric nanoparticles as an antifungal drug carrier. Amphotericin B (AmB), a natural antibiotic, was incorporated into the polymeric nanoparticles. The physical properties of AmB-incorporated polymeric nanoparticles with PCL-*b*-PDMAEMA and PCL-*b*-PEG were studied in relation to morphology and particle size. In the aggregation state study, AmB-incorporated PCL-*b*-PDMAEMA nanoparticles exhibited a monomeric state pattern of free AmB, whereas AmB-incorporated PCL-*b*-PEG nanoparticles displayed an aggregated pattern. In *in vitro* hemolysis tests with human red blood cells, AmB-incorporated PCL-*b*-PDMAEMA nanoparticles were seen to be 10 times less cytotoxic than free AmB (5 μg/ml). In addition, an improved antifungal activity of AmB-incorporated polymeric nanoparticles was observed through antifungal activity tests using *Candida albicans*, whereas polymeric nanoparticles themselves were seen not to affect activity. Finally, *in vitro* AmB release studies were conducted, proving the potential of AmB-incorporated PCL-*b*-PDMAEMA nanoparticles as a new formulation candidate for AmB.

Keywords: Amphotericin B, infectious disease, nanoparticle, hemolysis, *Candida albicans*

*Corresponding author
D.H.K.
Phone: +82-55-360-3870; Fax: +82-55-360-3879;
E-mail: sulsulpul@yahoo.co.kr
Y.-I.J.
Phone: +82-55-360-3873; Fax: +82-55-360-3879;
E-mail: nanomed@naver.com

Amphotericin B (AmB), an amphoteric macrocyclic natural antibiotic, is known to bind strongly to sterol components, such as ergosterol, in susceptible fungal cell membranes and to induce changes in permeability that can substantially induce lethal cell injury [10, 12, 24]. Since AmB has a broad antifungal spectrum activity, it is one of the first considerations for standard antibiotic therapy when faced with life-threatening fungal infections, such as visceral leishmaniasis and mucocutaneous leishmaniasis, amongst others [3]. Although there are well-known side effects of AmB, such as nephrotoxicity, which limit its clinical usage, AmB is also a useful antibiotic for the treatment of systemic fungal infections [7]. Other major drawbacks of AmB include poor aqueous solubility and its amphiphilic properties [2, 6]. Owing to its amphiphilic nature, AmB can easily be aggregated in an aqueous solution in a micellar form, and it is known that the toxic side effects of AmB are closely related to its aggregated form [2]. For this reason, AmB should be completely solubilized in an aqueous solution in a monomeric state to make it therapeutically active and less cytotoxic to the human body. Commercially available Fungizone®, a colloidal dispersion of AmB in sodium deoxycholate, has acute

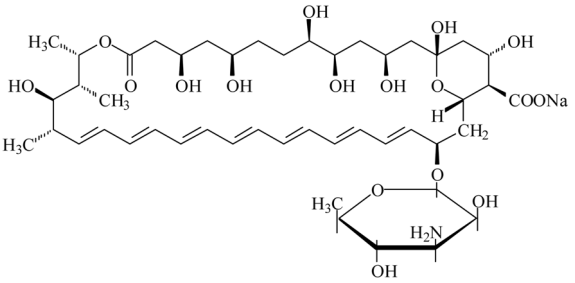

Fig. 1. Chemical structure of amphotericin B.

toxic side effects and has proved less effective on immunocompromised patients [9]. Liposome preparations of AmB (Amphotec™ and Abelcet®), also commercialized, are known to be less toxic than Fungizone® [21, 25]. Another candidate for AmB formulation is AmBisome®, a liposomal preparation. AmBisome® is known to be less toxic than other kinds of AmB liposomal formulations, and it is possible to increase the doses of AmB without correspondingly producing more pronounced toxic side effects. Larabi *et al* [18] reported that a lipid formulation of AmB exhibited reduced intrinsic toxicity *in vitro* and *in vivo*. Although many formulations of AmB are commercially available, it still remains a challenge to find a new formulation that reduces its toxicity.

In order to address this issue, we used a diblock copolymer for the preparation of AmB-incorporated core-shell type nanoparticles. Core-shell type nanoparticles have been reported as promising solubilizing agents of hydrophobic drugs, and favor drug delivery *via* a passive targeting mechanism, minimizing irritation at the injection site and toxic side effects. They have also been reported to have advantages when compared with conventional drug formulations such as emulsion preparations, liposomes and plain nanoparticles [16, 19]. Recently, we reported original synthesis of diblock copolymers (abbreviated as CD) composed of poly(ε-caprolactone) (PCL) and poly(*N,N*-dimethylamino-2-ethyl methacrylate) (PDMAEMA) *via* atom transfer radical polymerization (ATRP), which is one of the most robust controlled/"living" radical polymerization methods, using an optimized catalyst/ligand system [5]. PDMAEMA is a weak polybase polymer (pk_a ~7.0), which is soluble both at a neutral pH and in acidic medium, owing to protonation of the tertiary amine groups, and displays a well-marked polyelectrolyte behavior in water [22]. PDMAEMA (co)polymers have been extensively used as DNA binding agents either as pure compounds or as mixtures in nonviral systems, forming so-called polyplexes related to gene delivery systems, and are of particular interest in the field of gene therapy [8]. We hypothesized that the PDMAEMA component in the CD diblock copolymer would form the hydrophilic outer-shell of the core-shell type nanoparticles owing to its aqueous solubility, whereas PCL would form the inner core of the polymeric micelle because of its hydrophobic properties. To the best of our knowledge, this represents the first such formulation of AmB-incorporated CD nanoparticles prepared by ATRP.

In the present work, we studied the physical properties of AmB-incorporated nanoparticles with CD by way of comparison with PCL-*b*-methoxy poly(ethylene glycol) (abbreviated as CE) in relation to morphology, particle size, and aggregation states. Furthermore, examinations of the hemolysis and antimicrobial activities *in vitro*, in addition to drug release studies, were also conducted.

Materials and Methods

Materials

AmB and methoxy poly(ethylene glycol) (PEG, M_n=5,000 g/mol) were acquired from Sigma (St. Louis, USA). Dialysis membranes with a molecular weight cutoff (MWCO) of 8K and 12K g/mol were purchased from Spectra/Pro Membranes. Methanol (MeOH) and dimethyl sulfoxide (DMSO) were of HPLC grade and used without further purification. ε-Caprolactone (Acros), toluene (Labscan), and THF (Labscan) were dried over calcium hydride for 48 h at room temperature and distilled under reduced pressure prior to use. Aluminum triisopropoxide [$Al(O^iPr)_3$; Acros] was distilled under vacuum, quenched in liquid nitrogen, rapidly dissolved in dry toluene, and stored under a nitrogen atmosphere. The $Al(O^iPr)_3$ concentration was determined by back complexometric titration of Al^{3+} using the ethylenediaminetetraacetic acid (EDTA) disodium salt and $ZnSO_4$ at pH 4.8. 2-Bromo-2-isobutyryl bromide (Br^iBuBr; Aldrich), 1,1,4,7,10,10-hexamethylenetetramine (HMTETA; Aldrich) and copper(I) bromide (CuBr; Fluka) were used without further purification. *N,N*-(Dimethylamino-2-ethyl) methacrylate (DMAEMA; Aldrich) was passed through a column of basic alumina to remove the stabilizing agents and then stored under a nitrogen atmosphere at −20°C.

Synthesis of PCL-*b*-PEG (CE) Diblock Copolymers

The CE diblock copolymer was prepared as previously described [15]. Briefly, PEG and ε-caprolactone were mixed in a round-bottomed flask under vacuum. The mixture was cooled and degassed with a pump. The round-bottomed flask was then sealed off and placed in an oil bath at 180°C. After the polymerization was completed, the resulting product was cooled at room temperature and then dissolved in methylene dichloride. The solution was precipitated into an excess amount of cold ethanol and filtered to remove unreacted PEG homopolymer and ε-caprolactone monomers. The precipitates were washed with diethyl ether three times and then dried in a vacuum oven for 3 days.

Synthesis of Poly(ε-caprolactone)-*b*-PDMAEMA (CD) Diblock Copolymers

CD diblock copolymers were obtained by way of a three-step technique protocol as has previously been described [5, 22]. In a typical experimental run, all equipment was initially flame-dried, resulting in a clean airtight system. Particular attention was given to the bottom flask equipped with a three-way stopcock and a rubber septum. The flask was cleaned, dried, and then purged with nitrogen

before use as the polymerization vessel. ε-Caprolactone (30 ml, 0.27 mol) was added to 200 ml of freshly dried toluene. The solution was cooled to 0°C, and then 7.5 ml of the initiator solution [$Al(O^iPr)_3$, 0.83 M in toluene] was added. After 30 min, a few drops of an aqueous HCl solution (1 M) were added in order to stop polymerization. The polymer was then selectively precipitated in a large volume of cold heptane, filtrated, and dried under reduced pressure until a constant weight was observed. All residues were extracted by using the liquid/liquid extraction method, washing the polyester solution in chloroform once with an aqueous EDTA acid solution (0.1 M) buffered at pH 4.8 and then twice with water. The organic layer was finally poured into cold heptane to recover the α-isopropyloxy ω-hydroxy poly(ε-caprolactone) (PCL-OH) by precipitation. PCL-OH (30 g) was dissolved in 100 ml of THF with 3.8 ml of triethylamine. Br^{i}BuBr (3.4 ml) was then added dropwise to the solution. Triethylamine was used to trap the hydrobromic acid produced as an insoluble ammonium salt and thus completely displace the equilibrium. The reaction was carried out in a round-bottom flask under atmospheric pressure for 72 h at room temperature. Afterward, the PCL-Br in THF solution was filtered to remove the ammonium salt, precipitated in cold methanol, and then dried at 40°C. The CD diblock copolymers were synthesized by controlled ATRP of DMAEMA using the brominated macroinitiator (PCL-Br). For example CD-1 was prepared in THF at 60°C in the presence of a CuBr/HMTETA catalyst system under a nitrogen atmosphere. The system must be oxygen-free so as to prevent (poly)peroxide formation and transfer reactions. The catalytic system was placed in the system purged of oxygen by three repeated vacuum/nitrogen cycles. THF (10 ml) and the PCL-Br (1.75 g) initiator were placed in a second round-bottom flask, with nitrogen bubbling. The DMAEMA monomer (2.4 g) was injected into the first flask. The contents of the first flask were then transferred to the second flask. ([DMAEMA]/[PCL-Br]/[CuBr]/[HMTETA]=44/1/1/2). Following on from this, polymerization was carried out at 60°C for 5 h. The polymer solution was finally diluted in an excess of THF followed by the addition of cold heptane, resulting in precipitation. The copper catalyst system was extracted by passing the copolymer in the THF solution through a column of basic alumina. The purified copolymer solution was precipitated again in cold heptane, filtered, and then dried under reduced pressure at 40°C (yield 87%). Adjusting the initial amount of monomer in the reaction medium allowed for the modification of the length of the PDMAEMA segment.

Preparation of AmB-Incorporated Nanoparticles

Empty nanoparticles of CD or CE diblock copolymer were prepared as follows: 40 mg of block copolymer was dissolved in 5 ml of acetone. This solution was dropped into 20 ml of deionized water for 10 min to form nanoparticles and then stirred for an additional 10 min. This solution was introduced into a dialysis tube (MWCO of 8K g/mol) and dialyzed against deionized water for 24 h to remove solvent. Deionized water was exchanged at intervals of 1 h for 3 h and then exchanged at 3 h intervals for 21 h. Finally, the dialyzed solution was filter-sterilized with a 1.0-μm syringe filter and then lyophilized or analyzed.

AmB-incorporated nanoparticles were prepared as follows: 1 or 2 mg of AmB was dissolved in 2 ml of MeOH and this solution was then slowly dropped (0.1 ml for 10 min) into 10 ml of empty nanoparticle solution (4 mg polymer nanoparticles/ml distilled water). This solution was stirred gently for 30 min and the solvent was removed, under reduced pressure, using a rotary evaporator. To remove residual solvent, the solution was introduced into a dialysis tube and dialyzed against 1 L×10 of deionized water during 24 h by following the aforementioned purification procedure to purify and sterilize the AmpB-incorporated nanoparticles.

For evaluation of drug contents and loading efficiency, 5 mg of AmB-incorporated nanoparticles were dissolved in 10 ml of DMSO and further diluted 10 times with DMSO. The AmpB concentration was evaluated using a UV spectrophotometer (UV spectrophotometer 1201; Shimadzu Co., Japan) at 388 nm. Empty nanoparticles were used as a blank test.

$$\text{Drug contents} = \frac{(\text{drug weight in the nanoparticles})}{(\text{weight of nanoparticles})} \times 100$$

$$\text{Loading efficiency} = \frac{(\text{residual drug in the nanoparticles})}{(\text{initial feeding amount of drug})} \times 100$$

Morphology Analysis

The morphology of the nanoparticles was observed using a transmission electron microscope (TEM, JEOL JEM-2000 FX II, Japan). A drop of nanoparticle suspension containing phosphotungstic acid [0.05% (w/w)] was placed onto a carbon film coated on a copper grid for the TEM. The observation was done at 80 kV.

Particle Size Measurement

The particle size of the nanoparticles (1.0 mg/ml solution) was measured by photon correlation spectroscopy (PCS) (Zetasizer 3000; Malvern Instruments, UK) with an He–Ne laser beam at a wavelength of 633 nm at 25°C (scattering angle of 90°).

Aggregation State of AmB

For evaluation of aggregation properties in the nanoparticles, AmB was first dissolved in DMSO and diluted with deionized water [final DMSO concentration: 1% (v/v)]. Lyophilized nanoparticles, prepared as mentioned above, were reconstituted into deionized water and diluted with deionized water to a 5 μg AmB/mL concentration. Samples containing 5 μg/ml of AmB were used to measure UV spectra by a UV spectrophotometer.

***In Vitro* Drug Release Study**

The *in vitro* release experiment was carried out as follows: 5 mg of lyophilized nanoparticles of CD, or CE copolymer, was reconstituted into 5 ml of phosphate-buffered saline (PBS, 0.1 M, pH 7.4) and then introduced into a dialysis tube (MWCO of 12K g/mol). The dialysis tubes were placed in a 200-ml bottle with 95 ml of PBS, and the media stirred at 100 rpm at 37°C. At specific time intervals, the medium was taken for analysis of drug concentrations. Next, the whole medium was replaced with fresh PBS to prevent drug saturation. The medium was diluted 10~100 times with DMSO, and the concentration of the AmB released was determined using a UV spectrophotometer at 388 nm. The properties of the UV spectrum of AmB in DMSO did not change in the range of 0.1~10 μg/ml. Therefore, we diluted the release medium with DMSO to this range for drug concentration estimation using a UV spectrophotometer.

***In Vitro* Hemolytic Activity**

The hemolytic activity of the nanoparticles was evaluated by methods previously reported by Lavasanifar *et al*. [19]. Collected

human blood was centrifuged at 2,000 rpm, at 4°C, and the plasma eliminated. Red blood cells (RBCs) were washed with PBS (pH 7.4). AmB solutions and nanoparticle solutions were incubated with properly diluted RBCs at 37°C for 30 min and then cooled using an ice bath to stop hemolysis. After centrifugation at 14,000 rpm for 20 s, the supernatant was analyzed for hemoglobin at 576 nm using a UV spectrophotometer. For comparison, collected red blood cells were washed with PBS (pH 7.4) and lysed with a blood lysis buffer (pH 7.0, 1 mM EDTA) following centrifugation for hemoglobin analysis. The hemolytic activity of Amb and nanoparticles were expressed by comparison with this solution. The percentage of hemolysis was determined as follows:

$$\% \text{ hemolysis} = 100(ABS - ABS_0)/(ABS_{100} - ABS_0)$$

ABS=absorbance of the sample
ABS_{100}=absorbance at 100% hemolysis
ABS_0=absorbance at 0% hemolysis

Determination of Minimal Inhibitory Concentration

Candida albicans (KCTC 7270) was obtained from the Korean Collection for Type Cultures (KCTC). *C. albicans* was grown at 30°C in YM broth (yeast extract 3.0 g, malt extract 3.0 g, peptone 5.0 g, dextrose 10.0 g, per liter). AmpB was dissolved in DMSO and diluted further with phosphate-buffered saline (PBS, pH 7.2) to give a final concentration of 10 μg/ml. Empty or AmpB-incorporated nanoparticles were dissolved in distilled water and adjusted to the same final concentration (10 μg/ml). The fungal cells were seeded on a 96-well microtiter plate (Greiner, Nurtingen, Germany) in a YM broth at a density of 1×10^5 cells (100 ml per well). Serially diluted drugs (100 μl) were added to each well and the cell suspension was incubated for 24 h at 30°C. The inhibition of growth was determined by measuring the absorbance at 595 nm using a microtitration ELISA reader (Molecular Devices Emax, CA, U.S.A). The lowest concentration that completely inhibited growth of the fungal cells was defined as the minimal inhibitory concentration (MIC).

Results and Discussion

Charaterization of CE and CD Diblock Copolymer

A CE diblock copolymer was synthesized by a noncatalyzed ring-opening polymerization of ε-caprolactone in the presence of PEG. CD diblock copolymers were prepared following the three-step synthesis strategy summarized in Fig. 2. The first step was the ring-opening polymerization of ε-caprolactone, *via* the coordination-insertion mechanism initiated by $Al(O^iPr)_3$, to selectively form α-isopropyloxy ω-hydroxy poly(ε-caprolactone). The second step consisted of the conversion of PCL-OH into α-isopropyloxy ω-bromoisobutyrate poly(ε-caprolactone) macroinitiator (PCL-Br). The final step relied upon the ATRP polymerization of DMAEMA initiated by PCL-Br in THF at 60°C with CuBr/HMTETA as the catalytic/ligand system. ^{1}H-NMR and GPC characterization are summarized in Table 1.

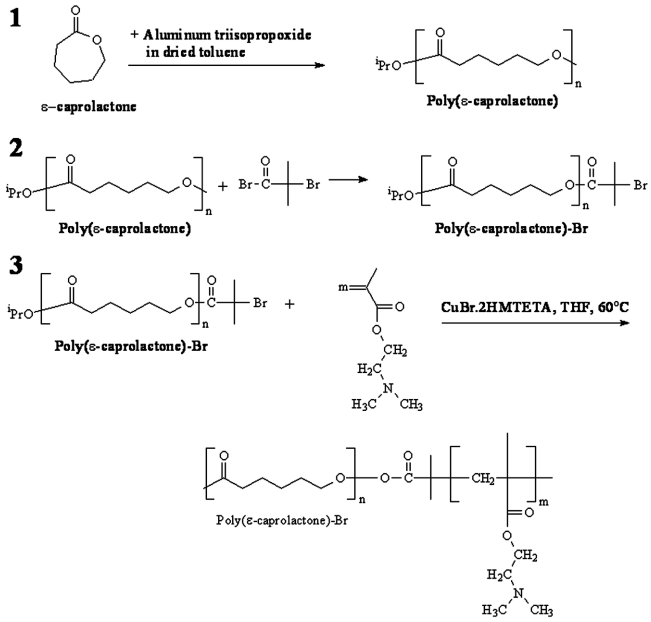

Fig. 2. Synthesis scheme for the CD diblock copolymer.

Preparation of AmpB-Incorporated Nanoparticles

AmB-incorporated nanoparticles were prepared by a partitioning of the drug into preformed nanoparticles following solvent evaporation and dialysis purification by the methods described above. The morphologies of resulting nanoparticles were observed using TEM as shown in Fig. 3. AmB-incorporated nanoparticles of CLE, CD-1,

Table 1. Molecular weight evaluations of CE and CD diblock copolymers.

	^{1}H NMR				GPC	Mw/Mn[b]
	M_n of PDMAEMA[a] (g/mol)	M_n of PCL-Br[a] (g/mol)	M_n of PCL (g/mol)	Total	$M_{n\ app\ GPC}$[b] (g/mol)	
CE[c]	-	-	4,250	9250	-	
CD-1	6,900	5,000		11,900	17,800	1.26
CD-2	10,800	5,000		15,800	21,900	1.24

[a]Number average mass (M_n) of PDMAEMA and PCL determined by ^{1}H NMR spectroscopy in $CDCl_3$.
[b]Apparent number average mass (Mn) and polydispersity index of block copolymers estimated by GPC in THF (+2 wt% NEt_3) with reference to polystyrene standards.
[c]In the case of CE diblock copolymer, M_n of PEG block was 5,000 g/mol (Sigma Co. Ltd., U.S.A.).

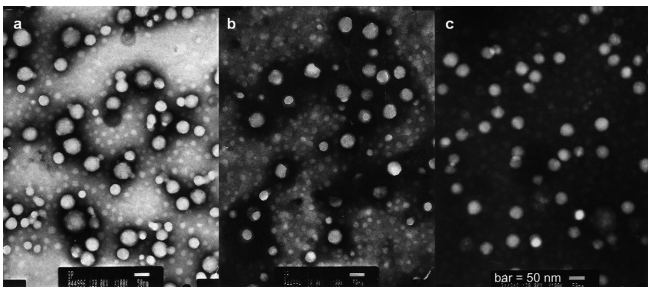

Fig. 3. Morphological observation of AmBCE (a), AmB-CD-1 (b), and AmB-CD-2 (c) nanoparticles by TEM.

and CD-2 nanoparticles, were seen to be spherical in shape in their morphology, and their size was observed to be between 30~100 nm. Their particle sizes from TEM images were not significantly different from the results of the latter particle size measurements (Fig. 3). The feeding amount of the drug was varied and different kinds of copolymer were used to incorporate AmB. As shown in Table 2, all formulations had a loading efficiency of more than 40% (w/w). In the case of CD-2, higher feeding amounts of AmB induced higher drug contents, but the loading efficiency correspondingly decreased. In the case of CE block copolymers, the loading efficiency of AmB was slightly higher than CD-2 nanoparticles. Interestingly, a higher drug content induced a larger particle size, indicating that increases of the drug in the nanoparticle's core might induce increases in particle size. Similarly, Choi *et al*. [6] reported that increases in drug contents induced increases of particle size. This tendency is also reported by several other authors [14, 15]. In particular, hydrophobic agents are known to form aggregates in the nanoparticle core at higher drug contents [11] and this phenomenon is thought to be related to the increase in particle size. We also observed that a higher PDMAEMA block length induced a lower loading efficiency of the drug. At all formulations, the loading efficiency was lower than expected. It may be difficult for the drug to penetrate into the inner core of the nanoparticles in water/methanol mixtures, and this fact may contribute to a decrease in loading efficiency. Although it was noted that increases in drug contents accordingly led to increases in particle size, it was observed that changes in PDMAEMA block length did not significantly affect the particle size. Compared with TEM observations, the average particle size of AmB-CD-2 nanoparticles measured by PCS was relatively larger. This result might be due to the fact that the PDMAEMA block may exist in a swollen state in an aqueous condition.

Aggregation State of AmB

The antifungal activity and toxicity of AmB is known to depend on its aggregation state [4, 13, 20, 23, 26]. When AmB is aggregated in an aqueous solution, it causes nonselective toxicity to the mammalian cells, and forms pores in mammalian cells and fungal cell membranes [4]. Furthermore, the aggregated form of AmB not only increases the intrinsic cytotoxicity against mammalian cells but also lowers the antimicrobial activity against microbial pathogens. On the other hand, the monomeric form of AmB is nontoxic to mammalian cells, whereas it causes leakage of fungal cells through selective interaction with ergosterol. In other words, monomeric AmB exhibited higher antimicrobial activity and less cytotoxicity than the aggregated form of AmB [6, 9, 21]. Fig. 4 and 5 illustrate the UV spectra of free AmB and AmB-incorporated polymeric micelle nanoparticles. The spectrum changed significantly according to the aggregation state of AmB. When AmB was present as a monomeric form in the DMSO, it exhibited an intrinsic UV spectrum, as shown in Fig. 4a. The absorption spectrum of free AmB is composed of four characteristic peaks, such as those seen at 350, 368, 388, and 412 nm. The aggregation status of AmB can be evaluated from these characteristic peaks.

When free AmB is in an aqueous solution, it must be severely aggregated and the spectrum is quite different, as seen in Fig. 4b. This aggregated state of free AmB in an aqueous environment is primarily characterized by a broad peak at 320~350 nm and three peaks between 350~420 nm. AmB-incorporated CE nanoparticles (AmB-CLE) exhibited a higher aggregation state, in aqueous solution, than free AmB when observed through the use of a UV spectrum (Fig. 4c). This might be due to the fact that AmB can be hydrophobically aggregated in the inner-core of the CE nanoparticles. UV spectrum analysis of AmB-CLE nanoparticles in DMSO had similar results to those of free AmB in DMSO (Fig. 4d). Compared with AmB-CD

Table 2. Characterization of amphotericin B-incorporated polymeric micelle of the CD block copolymer.

	Polymer/AmB weight ratio (mg/mg)	Drug contents (%, w/w)		Loading efficiency (%, w/w)	Particle size (nm)		
		Theoretical	Experimental		Intensity	Volume	Number
CE	48/2	4.0	2.3	57.5	97.5±36.3	89.6±28.3	81.0±20.1
CD-1	46/4	8.0	4.8	60.0	84.1±20.1	74.9±15.4	71.9±9.0
CD-2	48/2	4.0	2.1	52.5	67.6±15.1	64.1±12.3	56.3±8.4
	46/4	8.0	3.7	46.3	81.3±23.2	76.9±19.4	70.3±10.1

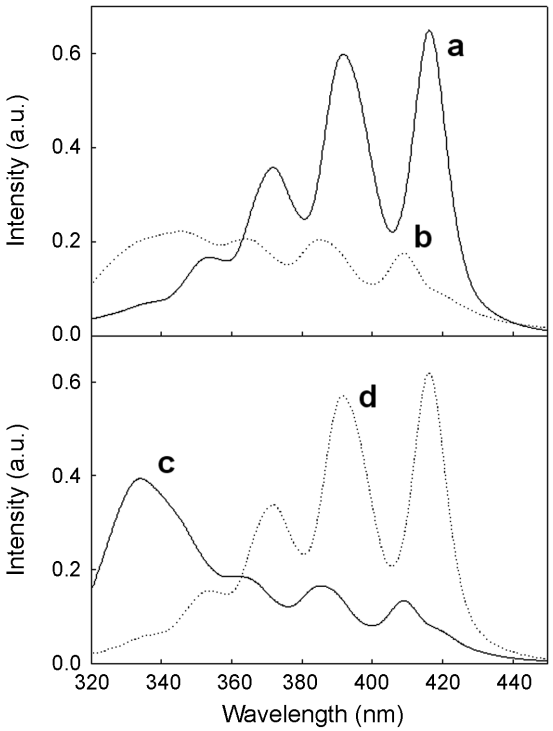

Fig. 4. UV spectrum analysis of free AmB and AmB-CLE nanoparticles.
Free AmB in DMSO (**a**) and distilled water [+DMSO 1.0% (v/v)] (**b**). AmB-CLE nanoparticles in water (**c**) and in DMSO (**d**). The AmB concentration was adjusted to 5.0 μg/ml.

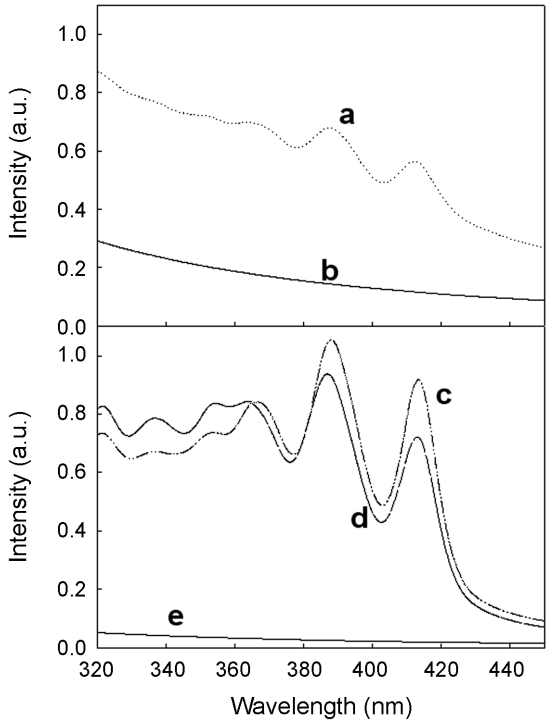

Fig. 5. UV spectrum analysis of AmB-CD nanoparticles.
AmB-CD-1 nanoparticles [drug contents: 4.8% (w/w)] (**a**) and empty CD-1 nanoparticles (**b**) in water. AmB-CD-2 nanoparticles [drug contents: 2.1% (w/w)] (**c**), [drug contents: 3.7% (w/w)] (**d**), and empty CD-2 nanoparticles (**e**) in water. The AmB concentration was adjusted to 5.0 μg/ml.

nanoparticles, AmB-CD-1 nanoparticles exhibited a similar spectrum in aggregated states, even if it appeared to be different from free AmB and AmB-CE nanoparticles. Specifically, the UV spectrum of AmB-CD-1 nanoparticles was seen to continuously increase until 320 nm. These results might be due to the intrinsic UV absorption properties of CD-1 nanoparticles, as shown in Fig. 5(b), whereas empty CD-2 nanoparticles have a relatively weak UV intensity. On the other hand, AmB-CD-2 nanoparticles in an aqueous solution displayed a different pattern in the UV spectrum (Fig. 5c and 5d) when compared with free AmB, AmB-CLE, and AmpB-CD-1 nanoparticles. They exhibited some similarities to a monomeric state of free AmB, as observed in DMSO (Fig. 4a) in the UV spectrum at 350~420 nm, even though the range of 320~350 nm in the UV spectrum is quite similar to that seen in the aggregated states. These results indicate that AmB-CD-2 nanoparticles may contribute to the decrease of aggregation of AmB in aqueous solutions even though some of them are aggregated in the nanoparticle core, as shown in Fig. 5(d). We suggest that the reason for a decreased aggregation of AmB in the case of AmB-CD-2 nanoparticles relies upon two factors. First of all, the lower drug contents of AmB-CD-2 nanoparticles can contribute to a decrease of AmB aggregation, and AmB is more likely to exist in a stage of molecular dispersion in the nanoparticle core. Generally, water-insoluble drugs aggregate and crystallize in the core of core-shell type nanoparticles with higher drug contents [11]. Adams *et al*. [1] reported that polymeric micelles composed of poly(ethylene oxide)-block-poly(β-benzyl-L-aspartate) were effective at decreasing intrinsic cytotoxicity and to increasing the antifungal activity of AmB [26]. In the latter report, they attained this efficacy of AmB-incorporated polymeric micelles through the control of the chain length of block copolymers. A derivative of this could be that longer hydrophilic chains, such as PDMAEMA blocks, may contribute towards the favorable solubilization of the drug into the nanoparticle core. It has also been reported that polymeric micelles composed of poly(ethylene glycol)-block-poly(ε-caprolactone-co-trimethylenecarbonate) could prevent the aggregation of AmB, and that the aggregation states of AmB could be changed by altering the preparation method, thus lowering cytotoxicity [23]. We also observed the prevention of AmB aggregation with CD block copolymer nanoparticles in an aqueous environment. As AmB-CE nanoparticles showed an aggregated pattern in the UV spectrum, further investigations were focused directly on the CD nanoparticles.

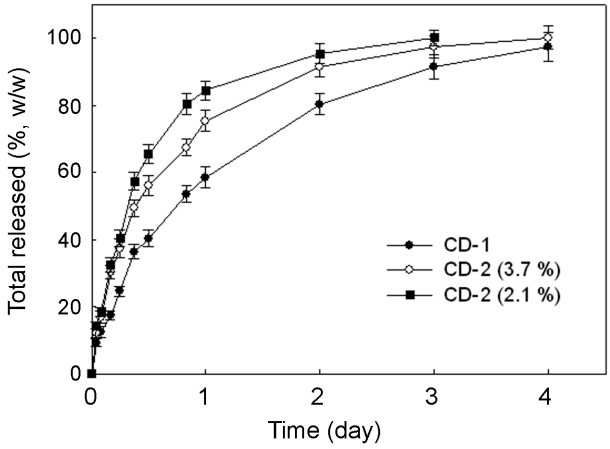

Fig. 6. Time course of drug release from CD-1 and CD-2 nanoparticles.

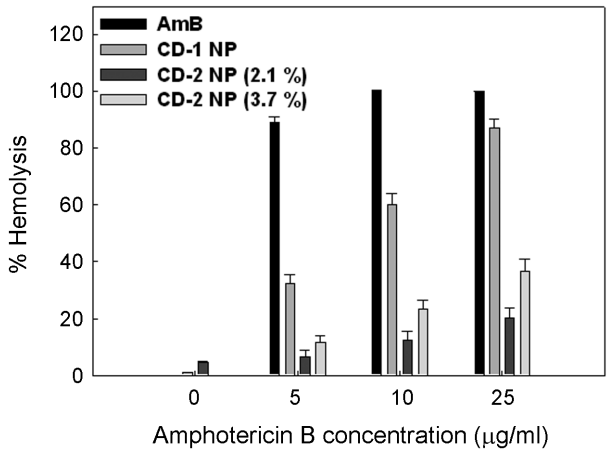

Fig. 7. Hemolytic activity of free AmB and AmB-CD nanoparticles.

At this time, the reason for the favorable aggregation of AmB in CD nanoparticles is not entirely clear. Bougard *et al*. [5, 27] reported that CD block copolymers form a self-organized structure in an aqueous solution in correspondence with physiological changes in the aqueous environment. Furthermore, the introduction of PDMAEMA blocks to the copolymers is known to impart hydrophilicity to the synthesized copolymers, allowing the copolymers to have favorable assembling properties in the physiological environment. We suggest that CD block copolymers may have favorable assembling properties with AmB, and hence their nanoparticles exhibit favorable physicochemical properties.

In Vitro Drug Release Study

Fig. 6 represents the release profile of AmB from AmB-CD nanoparticles in the outer aqueous phase. AmB-CD-2 nanoparticles exhibited a more than 70% (w/w) [drug contents 3.7% (w/w)] or 80% [drug contents 2.1% (w/w)] of drug release in 1 day, whereas AmB-CD-1 nanoparticles showed less than 60% of drug release. When using hydrophobic drugs, a similar phenomenon that higher drug loading contents give a slower release rate has been observed by several authors [11, 14, 17]. Since AmB is a hydrophobic drug, it can be aggregated in the nanoparticle core at higher drug contents due to the hydrophobic interaction, whereas molecular dispersion is expected at low drug contents. Molecular dispersion of the drug in the nanoparticles may induce a relatively faster release rate of the drug.

In Vitro Hmolytic Activity

Hemolysis was induced by different concentrations of AmB in order to evaluate the toxicity of AmB-CD nanoparticles. As shown in Fig. 7, free AmB treatment induced almost 90% hemolysis at 5 μg/ml, whereas nanoparticle treatment resulted in a lower than 40% hemolysis. In particular, AmB-CD-2 nanoparticles displayed very low hemolysis activity. In the case of AmB-CD-1 nanoparticles, hemolysis was seen to gradually increase according to increases in drug concentrations, and the extent of hemolysis became almost similar to that of free AmB treatment at 25 μg/ml. AmB-CD-2 nanoparticle treatment showed a lower hemolysis activity than AmB-CD-1 and free AmB treatment at all of the concentrations used with AmB-CD-2 nanoparticles exhibiting a lower than 40% hemolysis at 25 μg/ml. It is thought that the reason for a higher hemolysis activity for AmB-CD-1 nanoparticle treatment is due to the aggregated state of AmB in the nanoparticles. In the case of AmB-CD-2 nanoparticles, AmB exists in a monomeric state in the nanoparticles and this fact may be the reason for a lower hemolysis activity. Furthermore, AmB-CD-1 nanoparticle treatment in the low concentration range revealed a lower hemolytic activity than that of free AmB, even if the UV spectrum of AmB-CD-1 nanoparticles revealed a partially aggregated state of AmB. This result might be due to the sustained function of the polymeric micelle.

In Vitro Antifungal Activity

The antimicrobial activity of AmB-CD nanoparticles was evaluated with *Candida albicans* and the results are presented in Table 3. The MIC of AmB-incorporated nanoparticles was seen to be almost similar to that of free AmB, whereas empty nanoparticles had a significantly higher MIC value. This indicates that AmB-incorporated nanoparticles have a similar antimicrobial potential to free AmB itself, but that the polymer did affect the antimicrobial potential. The antimicrobial activity potential between AmB-CD-1 and AmB-CD-2 did not significantly change, although the hemolytic activity was noted as being quite

Table 3. Effects of free AmpB and AmpB-encapsulated nanoparticles on the MIC against *C. albicans*.

	MIC (μg/ml, n=3)
Free AmpB	0.673
AmpB-encapsulated polymeric micelle	
CD-1	0.73–1.3
CD-2	0.659–1.12
Empty polymeric micelle	
CD-1	≥11.0
CD-2	≥12.0

different. From these results, AmB-CD nanoparticles can be considered as superior candidates for the role of antimicrobial drug carriers.

In conclusion, diblock copolymers composed of PCL and PDMAEMA were synthesized, *via* the controlling ring-opening and ATRP methods, in order to produce effective drug delivery vehicles for AmB. AmB was incorporated into the polymeric nanoparticles of CD and CE block copolymers. The UV spectrum of AmB-CLE nanoparticles showed an aggregated pattern of free AmB, whereas AmB-CD nanoparticles exhibited a monomeric configuration. In preliminary *in vitro* studies, AmB-CD nanoparticles displayed a lower cytotoxicity, and similar antifungal activity, as that of free AmB. This means that the aggregation of AmB was prevented in the CD nanoparticles. Increases in the molecular weight of PDMAEMA resulted in increases in the observed effectiveness. This study has thus shown the potential of CD diblock copolymers as promising candidates for the prevention of aggregation in AmB formulation.

Acknowledgment

This study was supported by a grant of the Korean Healthcare Technology R&D Project, Ministry of Health and Welfare, Republic of Korea (Project No. A091047).

Abbreviation

CD, poly(ε-caprolactone)-block-poly(*N,N*-dimethylamino-2-ethyl methacrylate): CE, poly(ε-caprolactone)-block-poly(ethyleneglycol); AmB, amphotericin B

References

1. Adams, M. L. and G. S. Kwon. 2003. Relative aggregation state and hemolytic activity of amphotericin B encapsulated by poly(ethylene oxide)-block-poly(*N*-hexyl-L-aspartamide)-acyl conjugate micelles: Effects of acyl chain length. *J. Control. Release* **87:** 23–32.
2. Barwicz, J., S. Christian, and I. Gruda. 1992. Effects of aggregation of amphotericin B on its toxicity to mice. *Antimicrob. Agents Chemother*. **36:** 2310–2315.
3. Berman, J. D. 1997. Human leishmaniasis: Clinical, diagnostic and chemotherapeutic developments in past 10 years. *Clin. Infect. Dis.* **24:** 684–703.
4. Bolard, J., P. Legrand, F. Heitz, and B. Cybulska. 1991. One-sided action of amphotericin B on cholesterol-containing membranes is determined by its self-association in the medium. *Biochemistry* **30:** 5707–5715.
5. Bougard, F., M. Jeusette, L. Mespouille, P. Dubois, and R. Lazzaroni. 2007. Synthesis and supramolecular organization of amphiphilic diblock copolymers combining poly(*N*,*N*-dimethylamino-2-ethyl methacrylate) and poly(ε-caprolactone). *Langmuir* **23:** 2339–2345.
6. Choi, K. C., J. Y. Bang, P. I. Kim, C. Kim, and C. E. Song. 2008. Amphotericin B-incorporated polymeric micelles composed of poly(D,L-lactide-*co*-glycolide)/dextran graft copolymer. *Int. J. Pharm.* **355:** 224–230.
7. Deray, G. 2002. Amphotericin B nephrotoxicity. *J. Antimicrob. Chemother*. **49:** 37–41.
8. Deshpande, M. C., M. C. Davies, M. C. Garnett, P. M. Williams, D. Armitage, L. Bailey, M. Vamvakaki, S. P. Armes, and S. Stolnik. 2004. The effect of poly(ethylene glycol) molecular architecture on cellular interaction and uptake of DNA complexes *J. Control. Release* **97:** 143–156.
9. Dupont, B. 2002. Overview of the lipid formulations of amphotericin B. *J. Antimicrob. Chemother.* **49(Suppl S1):** 31–36.
10. Gallis, H. A., R. H. Drew, and W. W. Pickard. 1990. Amphotericin B: 30 years of clinical experience. *Rev. Infect. Dis.* **12:** 308–329.
11. Gref, R., Y. Minamitake, M. T. Peracchia, V. Trubetskoy, V. Torchilin, and R. Langer. 1994. Biodegradable long-circulating polymeric nanospheres. *Science* **263:** 1600–1603.
12. Groll, A. H. and T. J. Walsh. 2001. Uncommon opportunistic fungi: New nosocomial threats. *Clin. Microbiol. Infect.* **7(Suppl 2):** 8–24.
13. Ichinose, K., N. Tomiyama, M. Nakashima, Y. Ohya, M. Ichikawa, T. Ouchi, and T. Kanematsu. 2000. Antitumor activity of dextran derivatives immobilizing platinum complex (II). *Anticancer Drugs* **11:** 33–38.
14. Jeong, Y. I., J. B. Cheon, S. H. Kim, J. W. Nah, Y. M. Lee, Y. K. Sung, T. Akaike, and C. S. Cho. 1998. Clonazepam release from core-shell type nanoparticles *in vitro. J. Control. Release* **5:** 169–178.
15. Jeong, Y. I., M. K. Kang, H. S. Sun, S. S. Kang, H. W. Kim, K. S. Moon, K. J. Lee, S. H. Kim, and S. Jung. 2004. All-*trans*-retinoic acid release from core-shell type nanoparticles of poly(ε-caprolactone)/poly(ethylene glycol) diblock copolymer. *Int. J. Pharm.* **273:** 95–107.
16. Kataoka, K., G. S. Kwon, M. Yokohama, T. Okano, and Y. Sakurai. 1993. Block copolymer micelles as vehicles for drug delivery. *J. Control. Release* **24:** 119–132.
17. Kwon, G. S., M. Naito, M. Yokoyama, T. Okano, Y. Sakurai, and K. Kataoka. 1995. Physical entrapment of adriamycin in AB block copolymer micelles. *Pharm. Res*. **12:** 192–195.
18. Larabi, M., V. Yardley, P. M. Loiseau, M. Appel, P. Legrand, A. Gulik, C. Bories, S. L. Croft, and G. Barrat. 2003. Toxicity and antileishmanial activity of a new stable lipid suspension of

amphotericin B. *Antimicrob. Agents Chemother.* **47:** 3774–3779.
19. Lavasanifar, A., J. Samuel, S. Sattari, and G. S. Kwon. 2002. Block copolymer micelles for the encapsulation and delivery of amphotericin B. *Pharm. Res*. **19:** 418–422.
20. Legrand, P., E. Romero, J. P. Devissaguet, C. B. Eleazar, and J. Bolard. 1992. Effects of aggregation and solvent on toxicity of amphotericin B to human erythrocytes. *Antimicrob. Agents Chemother*. **36:** 2518–2522.
21. Mouton, J. W., D. T. Te Dorsthorst, J. F. Meis, and P. E. Verweij. 2009. Dose-response relationships of three amphotericin B formulations in a non-neutropenic murine model of invasive aspergillosis. *Med. Mycol*. **29:** 1–7.
22. Shim, Y. H., F. Bougard, R. Lazzaroni, and P. Dubois. 2008. Synthesis and aqueous solution properties of 2-(dimethylamino)ethyl methacrylate based (co)polymers: Viscometric and AFM analysis. *Eur. Pol. J.* **44:** 3715–3723.
23. Vandermeulen, G., L. Rouxhet, A. Arien, M. E. Brewster, and V. Preat. 2006. Encapsulation of amphotericin B in poly(ethylene glycol)-block-poly(ε-caprolactone-co-trimethylenecarbonate) polymeric micelles. *Int. J. Pharm*. **309:** 234–240.
24. Walsh, T. J., J. Hiemenz, and E. Anaissie. 1996. Recent progress and current problems in treatment of invasive fungal infections in neuropenic patients. *Infect. Dis. Clin. North Am.* **10:** 365–400.
25. Yardley, V. and S. J. Croft. 1997. Activity of liposomal amphotericin B against experimental cutaneous leishmaniasis. *Antimicrob. Agents Chemother*. **41:** 752–756.
26. Yu, B., T. Okano, K. Kataoka, S. Sardari, and G. Kwon. 1998. *In vitro* dissociation of antifungal efficacy and toxicity for amphotericin B-loaded poly(ethylene oxide)-block-poly(beta-benzyl-L-aspartate) micelles. *J. Control. Release* **56:** 285–291.
27. Bougard, F., C. Giacomelli, L. Mespouille, R. Borsali, Ph. Dubois, and R. Lazzaroni. 2008. Influence of the macromolecular architecture on the self-assembly of amphiphilic copolymers based on poly(*N*,*N*-dimethylamino-2-ethyl methacrylate) and poly(ε-caprolactone). *Langmuir* **24:** 8272–8279.
28. Spasova, M., L. Mespouille, O. Coulembier, D. Paneva, N. Manolova, I. Rashkov, and P. Dubois. 2009. Amphiphilic poly(D- or L-lactide)-b-poly(*N*,*N*-dimethylamino-2-ethyl methacrylate) block copolymers: Controlled synthesis, characterization, and stereocomplex formation. *Biomacromolecules* **10:** 1217–1223.